IEEE Access
Multidisciplinary | Rapid Review | Open Access Journal

SPECIAL SECTION ON GNSS, LOCALIZATION, AND NAVIGATION TECHNOLOGIES

Received June 4, 2018, accepted July 9, 2018, date of publication July 26, 2018, date of current version August 15, 2018.

Digital Object Identifier 10.1109/ACCESS.2018.2856521

Positioning Performance Assessment of Geodetic, Automotive, and Smartphone GNSS Receivers in Standardized Road Scenarios

ANDREJ ŠTERN AND ANTON KOS, (Senior Member, IEEE)
Faculty of Electrical Engineering, University of Ljubljana, 1000 Ljubljana, Slovenia

Corresponding author: Andrej Štern (andrej.stern@fe.uni-lj.si)

This work was supported in part by the European COST Action: Satellite Positioning Performance Assessment for Road Transport through the Short Term Scientific Mission to Nantes, France, under Grant TU1302 and in part by the Slovenian Research Agency through algorithms and optimization methods in telecommunications under Grant P2-0246.

ABSTRACT Intelligent transport system applications use the global navigation satellite systems (GNSSs) to deliver the information on position, velocity, and time. With the expected deployment of critical road services, GNSS-based positioning terminals will have to be sufficiently accurate and their service will have to be available under any environmental condition. As the answer to the absence of standards and certification procedures of positioning terminals in road transport services, the European COST Action SaPPART was launched and the European norm EN 16803-1 was accepted. They provide the methodology and the guidelines for the terminal performance assessment. Section I presents the data collection methodology based on European norm EN 16803-1 with the definition of performance metrics and classification, operational scenarios, standardized GNSS environments, and field test guidelines. It is followed by the description of the measurement setup, including the trajectories, experimental vehicle with a reference trajectory system, and 17 tested GNSS receivers. The performance assessment of geodetic, automotive, and smartphone GNSS receivers was carried out through the extensive data collection campaign in Nantes, France. The campaign covered four types of environments: clear-sky, rural, peri-urban, and urban. The presented results focus on the basic performance features of accuracy, availability, and the classification of positioning terminals according to SaPPART methodology. The final conclusion is that for achieving a sub-meter accuracy at 95% confidence level in mixed road scenarios, a hybrid multi-sensor positioning approach is required for the majority of mass-market receivers.

INDEX TERMS Satellite navigation systems, intelligent transportation systems, standardization, accuracy, availability, performance evaluation.

I. INTRODUCTION

Global Navigation Satellite System (GNSS) has become a ubiquitous technology with prevalent use in Location Based Services (LBS) using smartphones, followed by road sector with professional applications that are expected to dominate all other market segments in terms of cumulative revenue in the forecasting period 2015-2025. Also, new services emerge where GNSS is considered as the catalyst for the diversity of use cases, e.g., Internet of Things, Big Data, mHealth, Augmented Reality, Smart Cities, and Multimodal Logistics [1]. Autonomous vehicles, as one of the cases of many automotive research topics and policy makers [2], will surely benefit from GNSS in combination with multitude of other sensors and connectivity, merging all these technological areas into mobility and Intelligent Transport System (ITS) services.

Positioning systems like GNSS provide a set of information, including Position, Velocity, and Time (PVT). These basic quantities require additional application module (Fig. 1) [3] that transforms their values into high-level application quantities and, finally, to provide the user services. For instance, the Personal Navigation Device (PND) provides navigation services in form of a guidance on the embedded display, where the application inside the device performs map-matching, guidance information retrieval, and user information generation, all based on the PVT input. The End-to-End (E2E) performance of such service depends on the performance of each chain element, from GNSS onwards.

The most demanding ITS services are considered as *safety-critical.* [4], because their failure may result in causing harm to humans, destruction of the system, and damage to

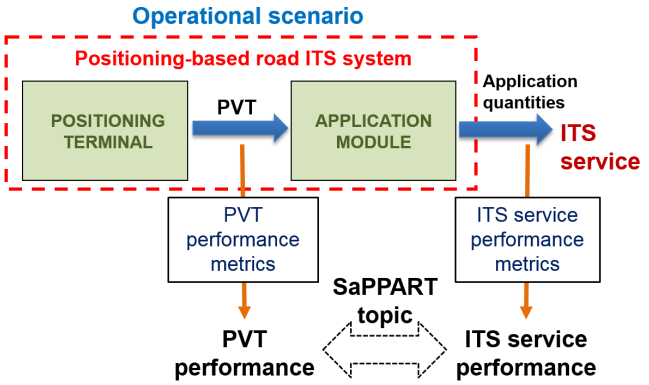

FIGURE 1. The breakdown of a road ITS system into its main components according to SaPPART.

property or the environment. Some examples of such applications are: Cooperative ITS (C-ITS) with surroundings awareness [5], Advanced Driver Assistance Systems (ADAS) [6], and autonomous driving [7].

The degradation of *liability-critical* applications may result in significant economic consequences, e.g., during GNSS-based Road User Charging (RUC) [8] and insurance telematics with services like Pay-How-You-Drive [9], [10]. The *regulated* applications, as the third sensitive group, might pose some legal issues, e.g., at establishing automated emergency calls (eCall in Europe, E911 in United States, and ERA-GLONASS in Russia) [11], and securing enhanced digital or smart tachographs [12]. All these do need to apply additional mechanisms for the quality assessment of PVT quantities in order to assure they meet the required performances.

It is known that the reception of weak GNSS signals at the GNSS-Based Positioning Terminals (GBPT) and their conversion to PVT suffer from a variety of impact factors, resulting in a degraded positioning performance. The PVT errors arise from the satellite configuration (orbital errors, clock bias), signal propagation (ionospheric and tropospheric refraction, scintillation), receiver noise (clock bias, antenna phase center variations), receiver's global location (the geometrical distribution of the visible satellites), and local environment (multipath, deep fast fading, limited satellite visibility, RF noise) [13]–[18]. The accumulated error is highly variable reaching from several meters to over 1000 meters on the pseudo-ranges in urban canyons [19] due to numerous reflections of signals causing multipath effects.

Some of these errors can be mitigated using multi-constellation [20]–[23] and multi-frequency receivers [24], multipath rejection antenna designs [25] or Real-Time Kinematic (RTK) techniques [26]. In September 2017 a mobile devices chipset manufacturer announced the first mass-market combined E1/L1 and E5/L5 receivers that will be able to provide lane-level accuracy of 30 cm by applying ionospheric corrections from GPS and Galileo [27]. This can introduce completely new services to the LBS market and enable smartphones to play an important role in the road ITS aftermarket segment.

A variety of positioning terminals with different performances will require assessment procedures during certification processes. Especially for critical services, the GBPTs have to be matched against the performance classes that should put trust in the delivered PVT. During the last two decades the main motivator behind these processes was civil aviation [28]–[30], while the road related GNSS standardization evolved at much slower pace.

The European organization CEN-CENELEC has approved the first part of standard EN 16803 titled "Use of GNSS-based positioning for road Intelligent Transport Systems" [31], providing identification and definitions of positioning performance features and metrics that characterize the GBPT performance requirements. These have to match a certain operational scenario, i.e. the conditions in which the GBPT is operating that may have a huge impact on its performances.

As a supporting activity to the standardization, the European COST Action "TU1302 - Satellite Positioning Performance Assessment for Road Transport (SaPPART)" [32] delivered the White paper [4], Handbook [3], and Guidelines [33], defining a comprehensive framework for the assessment of performances of GBPTs used in ITS and personal mobility applications [34].

This paper focuses on the SaPPART field test data collection campaign using a set of geodetic, automotive, and smartphone GBPTs in standardized GNSS environments with respect to the EN 16803-1 methodology and field test guidelines. The main contributions of this paper are:

1) An overview of position performance metrics based on the European standard EN 16803-1 and classification boundaries from COST Action SaPPART.
2) The characterization of standardized GNSS reference environments including field test guidelines for comparable performance results around the globe.
3) The description of professional field test set-up using an accurate RTMeS and 3 groups of GNSS receivers.
4) The accuracy and availability performance assessment and classification results for the whole set of GNSS receivers in 4 reference GNSS environments.

II. EUROPEAN STANDARDIZATION AND GNSS PERFORMANCE METRICS

The published standard EN 16803-1:2016 is titled "Definitions and system engineering procedures for the establishment and assessment of performances" [31]. This system engineering approach provides support for engineers facing the problem of handling the E2E performances of a GBPT based road ITS system along the system development. Fig. 1 presents the ITS system breakdown into two components: the GBPT and the road ITS application, linked by the interface for sharing the PVT information and possible extras, e.g., the integrity parameters.

These GBPT features are characterized by performance metrics, requiring detailed overview of GBPT outputs to which the different metrics will be defined, the characteristics

of those outputs that are relevant for the performance features identification, the performance features themselves, and the metrics definition, summarized in Fig. 2.

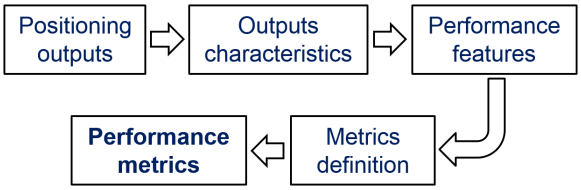

FIGURE 2. Positioning performance metrics workflow in EN 16803-1.

A. POSITIONING OUTPUTS AND CHARACTERISTICS

The widely used positioning quantities at the output of GBPT are the position, velocity, and time (PVT), still others might be of interest to the road ITS applications. It is quite uncommon to address these parameters directly by the performance metrics, rather their errors are observed.

The *position* is the location of GBPT, to be more exact, the antenna phase center given in specified reference frame and coordinate system. In the case of low cost receivers with National Marine Electronics Association (NMEA) output, the position components (longitude, latitude, and height) are expressed in WGS84 frame with geodetic coordinates e.g., latitude in GGA, RMC, and GLL sentences [35]. The metrics addresses rather their errors representing the difference between provided and true position.

The *velocity* is given relative to the ground as a three-component vector, typically expressed in Cartesian coordinate system centered at the user position (e.g., North, East, and Up directions). This parameter can be only found in proprietary sentences like Garmin PGRMV. The *speed* is a scalar value of the norm of velocity describing how fast the GBPT is moving irrespective of the direction. The NMEA uses a combination of speed and heading to deliver velocity information e.g., using the RMC and VTG sentences. Again, their errors are used during the performance assessment.

The *protection level* (PL) from integrity bounds the positioning or velocity error in real-time with a given high probability. Their performances are characterized in statistical sense evaluating their size which is directly linked to their usability for a specific application, and using the probability parameter that a PL fails to contain the error. This probability, known as *integrity risk*(IR), is application specific and set in advance following the service requirements. Since protection level parameters cannot be found in common NMEA sentences, their value is defined as infinite for the performance characterization purposes [3].

Additionally, the quality indicators may be provided at the output of GBPT. Among them, the *Dilution of Precision* (DOP) and *covariances* from the estimation process can be used (if available), but they are not considered to be sufficiently reliable measurements of performance [31].

Finally, the *timestamp* information indicates the time reference for all other quantities above. The usage of Coordinated Universal Time (UTC) standard is recommended and can be found in many NMEA sentences e.g., in RMC, GGA, GLL, and ZDA [35]. Since the *time of output* is considered as always posterior, the relation to the timestamp is called *output latency*.

B. POSITIONING PERFORMANCE FEATURES

The most relevant GNSS performance features, related to usage in road ITS scenarios, are accuracy, availability, continuity, and integrity [36]–[40].

The *accuracy* refers to a statistical characterization of the error in position, velocity or speed with respect to the ground truth. The *integrity* refers to the measure of trust that can be placed in the correctness of the position or velocity component of the information delivered. The *continuity* is the probability that the specified system performance (e.g., accuracy and integrity) will be maintained for the whole planned duration of operation. The *availability* can be defined in terms of the percentage of time during which the output of interest is provided to the application module.

Additionally, several other performance features have been defined as an answer to modern threats, like jamming [41]–[43] and spoofing [44]–[46]. These are *robustness*, *reliability*, *timing,* and *authentication*, which are often a subject of a research [47]–[49].

The relation between most relevant performance features is summarized in literature review [40], presenting their relations in the form of navigation performance pyramid as outlined in Fig. 3. The performance hierarchy starts with accuracy, which is directly linked to integrity, because the lack of confidence in accuracy fails the integrity check. Further, the continuity is the probability that accuracy and integrity will be maintained for the whole planned duration. On the top of the pyramid the availability requires the specifications of all others to be met.

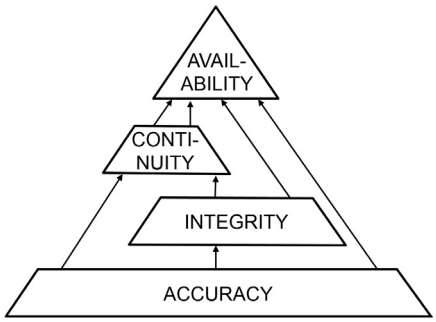

FIGURE 3. The hierarchy and relations between main performance features of navigation performance in the form of pyramid.

An example of Required Navigation Performance (RNP) for road and ITS applications is presented in Table 1 with impact scoring H - High, M - Medium, and L - Low [50].

C. POSITIONING PERFORMANCE METRICS

In order to quantify these features to match the required navigation performance, corresponding metrics must be introduced.

TABLE 1. Quantitative evaluation of performance requirements.

Road applications	Accuracy	Availability	Integrity	Continuity
Autonomous driving	H	M	H	H
Advanced navigation	M/H	M	H	H
Fleet management	L/M	H	H	L/M
Road charging	L/M	H	H	L
Insurance telematics	L	M	H	L/M
eCall services	M	H	M	L
Road navigation	M	H	M	L
Vehicle tracking	L	M	M/H	L

The accuracy is often described by the mean and standard deviation of the error distribution it refers to. This definition requires a known and well characterized error distribution, e.g., where errors can be defined with mean and standard deviation, as in the case of highway clear-sky scenario with multi-constellation receivers (Fig. 4a). Typical urban road environment suffers from heavy-tailed distributions [51] that may change the shape over time and place (Fig. 4b). Therefore using mean and standard deviation here does not capture the error characteristics of interest [3].

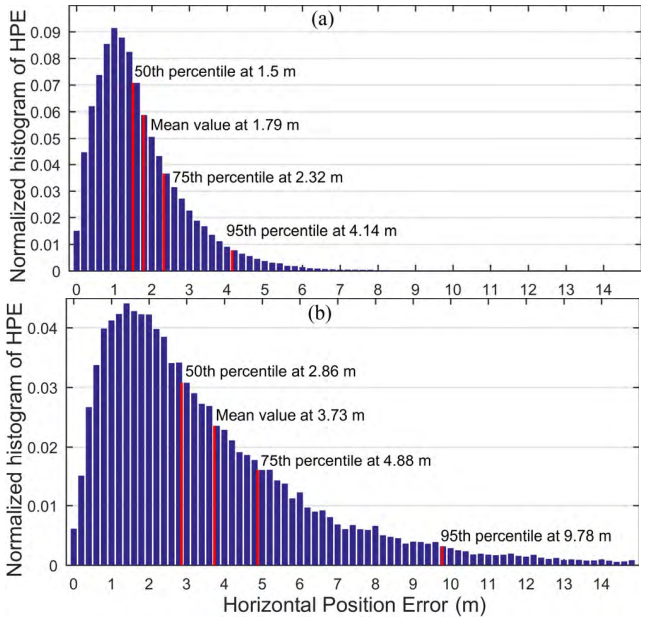

FIGURE 4. A comparison between Horizontal Position Error (HPE) distributions from (a) clear sky highway environment and (b) urban environment with visible heavy-tailed distribution.

The performance metrics in EN 16803-1 is characterized by CDF percentiles for accuracy, integrity, and timing, and additional percentages of operating time intervals (T) for availability. These performance features are further divided according to the GBPT output, e.g., to position accuracy, and these sub-features have associated metrics for each of their components. As an example, the position accuracy metrics is defined as the set of 3 statistical values given by the 50th, 75th, and 95th percentiles of the cumulative distribution along each direction or spatial combination, e.g., horizontal, 3D, east, north, along track, cross track, and vertical. Table 2 summarizes the performance metrics given in the 2016 release of EN 16803-1 [31].

TABLE 2. The summary of performance metrics, based on EN 16803-1.

Performance feature	Performance sub-feature	Component or type	Associated metrics
Accuracy	Position Velocity	3D Horizontal East / North Along track Cross track Vertical	50th, 75th, and 95th percentiles of the cumulative distribution of the component error
	Speed	None	
Integrity	Position PL Velocity PL	3D Horizontal East / North Along track Cross track Vertical	50th, 75th, and 95th percentiles of the cumulative distribution of PL computed for the target integrity risk
Availability	Position Velocity Speed	None	The percentage of operating time intervals of length T containing at least one parameter output
Timing	Timestamp resolution	None	The value of the least significant bit for timestamp encoding
	Output latency stability Output rate stability	None	50th, 75th, and 95th percentiles of the cumulative distribution of the variable error
	Time To First Fix	Cold start Warm start Hot start	50th, 75th, and 95th percentiles of the cumulative distribution of the elapsed time until a valid position solution

D. POSITIONING PERFORMANCE CLASSIFICATION

While the EN 16803-1 defines the performance metrics, it does not provide strict requirements that will formalize the performance expectations for a certain operational scenario. This classification methodology is provided in SaPPART Guidelines [33] in a form of three distinct classes for horizontal accuracy, visualized in Fig. 5. The same methodology can be used for all the performance features where the associated metrics is expressed in 50th, 75th, and 95th percentiles of the cumulative distribution. The coordinates of intersection percentiles for the horizontal accuracy are presented in the classification proposal in Table 3. Since the boundary values are based on several GBPT field tests and agreed among SaPPART field experts, they are considered as the technology perspective values.

It is expected that Class 1 members reside from accurate geodetic receivers operating in relatively clear-sky environments, Class 2 from the majority of mass-market and automotive receivers with roof-mounted antenna operating under same unobstructed conditions, and Class 3 for the receivers with integrated antenna placed inside the vehicle (e.g., smartphones), older generations of Class 2 receivers or regular

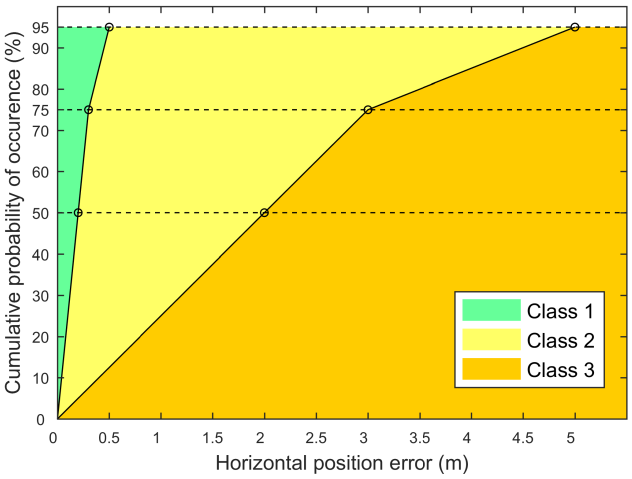

FIGURE 5. Horizontal accuracy performance classification from the technology perspective as proposed by COST Action SaPPART.

TABLE 3. horizontal accuracy performance classification boundaries from the technology perspective [3].

Class	P = 50th percentile	P = 75th percentile	P = 95th percentile
Class 1	P ≤ 0.2 m	P ≤ 0.3 m	P ≤ 0.5 m
Class 2	0.2 m < P ≤ 2.0 m	0.3 m < P ≤ 3.0 m	0.5 m < P ≤ 5.0 m
Class 3	P > 2.0 m	P > 3.0 m	P > 5.0 m

Class 2 devices operating in constrained environments like modern urban [33], [52].

Another type of horizontal accuracy classification presented in Table 4 is from the point of view of road applications. The main idea here is based on different application requirements and not the technological performance of GNSS or hybridized receivers. The names of accuracy classes reside from the parts of a roadway: In-lane, Lane, Carriageway, Area, and No specific [7], [33]. The No specific coarse class does not require any special accuracy performance, but should provide a valid GNSS position.

TABLE 4. Accuracy performance classification boundaries - the applications' perspective [7], [33].

Class	Class name	P = 50th percentile	P = 75th percentile	P = 95th percentile
1	In-lane	P ≤ 0.1 m	P ≤ 0.15 m	P ≤ 0.25 m
2	Lane	0.1 m < P ≤ 0.4 m	0.15 m < P ≤ 0.6 m	0.25 m < P ≤ 1.0 m
3	Carriageway	0.4 m < P ≤ 4.0 m	0.6 m < P ≤ 6.0 m	1.0 m < P ≤ 10.0 m
4	Area	4.0 m < P ≤ 40 m	6.0 m < P ≤ 60 m	10.0 m < P ≤ 100 m
5	No specific	P > 40 m	P > 60 m	P > 100 m

During the GBPT performance assessment procedure it is likely that some classification results switch the classes at probability points. For example: a GBPT can reach Class 1 requirements at 50th and 75th percentile, but reaches only Class 2 at 95th percentile. In this case the decision on the final class is based on the worst case, i.e. the maximum class value, so the GBPT is characterized as Class 2 receiver.

Other sources of horizontal accuracy classification provide different class boundaries and counts, e.g., "Which road" with typical accuracy better than 5 m, "Which lane" with better than 1.5 m, and "Where in lane" with the typical requirement 1 meter or better [53]. Clausen *et al.* [37] summarized rough requirements for the same classes as 5 m, 1.1 m to 1.5 m, and 0.5 m to 1.0 m, respectively. Stephenson *et al.* [54] proposed an addition of more accurate horizontal accuracy class "Active Control" with strict requirement better than 0.1 m, i.e. the same as the class In-lane at 50th percentile in [7].

The classification of position availability is based on metrics, presented in Table 2. The SaPPART's Handbook [3] and Guidelines [33] provide the availability classes using the percentage boundaries of availability intervals T, during which the GBPT provides at least one position output (Table 5). The parameter T can be adjusted to the application requirements, e.g., $T = 60$ s for parking fees on a per-minute basis and new classes can be defined according to the charging loss risk.

TABLE 5. Availability performance classification boundaries as proposed by COST action SaPPART.

Class	A = Availability (T)
Class 1	A > 99%
Class 2	95% < A ≤ 99%
Class 3	A ≤ 95%

The classification of integrity parameters PL availability, PL size, and integrity risk can be found in [33]. Considering one application that uses metrics on multiple performance features, the overall performance of the GBPT can be represented by a multi-parametric label that will be representative of its behavior in a given environment [33].

E. EMERGING STANDARD RELEASES

Three different parts of EN 16803 have been defined, but only the first part has been released till early 2018. While part 1 theoretically addresses the assessment of the road ITS system performance from the GBPT perspective, provides the definitions of performance features and metrics, and characterizes the operational scenario, the upcoming parts 2 and 3 focus more on field testing and potential threats [31].

The EN 16803-2: "Assessment field tests for basic performances of GNSS-based positioning terminals" will propose field testing procedures to assess the GBPT performances for different use cases described by an operational scenario. Three types of testing procedures will be considered: field, laboratory, and record & replay, using PVT error models and Software Defined Radio (SDR).

The EN 16803-3: "Assessment field tests for security performances of GNSS-based positioning terminals" will focus on the performances of GBPT under intentional or non-intentional interferences in terms of robustness, specifying

detection and mitigation procedures as an answer to jamming and spoofing attacks.

III. OPERATIONAL SCENARIOS AND FIELD TESTS GUIDELINES

The operational scenario is a set of conditions, influencing the performance of GBPT and the whole road ITS system. These conditions must be described sufficiently in order to equally assess the performances of different positioning terminals at different locations across the globe. The EN 16803-1 [31] proposes the threefold structure of operational scenarios as presented in Fig. 6.

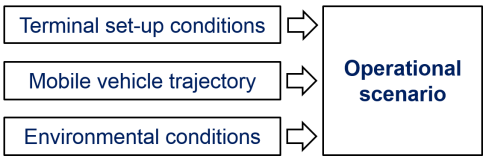

FIGURE 6. The structure of operational scenario posing a great influence upon GBPT performance.

The terminal set-up conditions comprise the installation of GBPT in the vehicle, focusing on the GNSS antenna part. Here, the characteristics of antenna, the mounting location, and possible attenuations and obstructions of windshield and vehicle metal body should be described in detail [55].

The mobile vehicle trajectory incorporates a series of time-stamped positions and driving dynamics. Since every driven trajectory is unique, it can be characterized by common parameters, e.g., minimum and maximum speed, and accelerations.

The environmental conditions are based on the variable GNSS constellation visibility (changing accuracy and availability) [56], the latitude of the test location (the visible portion of GNSS constellation, dilution of precision) [56], the geometry of surrounding static and dynamic obstacles (mountains, buildings, and vegetation) with their physical properties (causing reflections and attenuations) [37], the electromagnetic environment (natural or man-made RF noise) [57], the atmospheric weather conditions (absorbing deep fog and heavy rain, reflecting snow) [58], and ionospheric conditions (delays, refractions, scintillations) [59]. Since these environmental conditions heavily affect the changing GBPT performance, the EN 16803-1 introduces and characterizes a new category, the GNSS environment.

A. GNSS REFERENCE ENVIRONMENTS

Field tests results from different locations can be compared only with the common agreement on the GNSS environment belonging to the same well defined category. In EN 16803-1 [31] 6 high-level reference environment categories are defined, based on elementary environmental conditions:

1) Flat Rural: rural clear-sky countryside roads and highways with Line-of-Sight (LOS) propagation and masking angles smaller than 10°;
2) Tree-lined Rural: rural roads with strong foliage attenuation effects, LOS propagation, and masking angles smaller than 10°;
3) Mountainous: roads surrounded by high hills and mountains generally on one side of the road, occasional tunnels and trees, masking angles up to 80°, and occasional Non-Line-of-Sight (NLOS) phenomena;
4) European Peri-urban: medium cities' ring roads with relatively large streets and medium height buildings, masking angles up to 30°, and occasional NLOS phenomena;
5) European Urban: narrow streets, large avenues or ring roads in European old big cities with building height from medium to tall, masking angles up to 60° causing frequent NLOS phenomena;
6) Modern Urban Canyon: modern cities with high buildings constructed mainly of glass and metal, many tunnels, and masking angles over 60° causing frequent NLOS phenomena.

B. FIELD TEST GUIDELINES

Performance assessment of the GBPT should comply with additional design specifications to minimize the effects of variable satellite visibility, ionospheric conditions, and to avoid situations with excessive biased data, not directly related to the reference environment [31]. These specifications are presented in a form of the field test guidelines and should be respected to the greatest extent.

The performance analyses should be based on a sufficient set of data, e.g., more than 2 hours at the output rate of at least 1 Hz while traveling with standard speed within the legislative limits. In case of traffic jams or frequent stopping at the traffic lights or intersections, the test acquisition should be prolonged by a cumulative time where speed is below 2 km/h. This is necessary especially in constrained environments with frequent multipath and NLOS, where the stationery nature of trajectory may additionally enlarge the positioning errors.

To minimize the effects of the changing constellation visibility, tests should be performed at least 3 times with a time interval between consecutive tests of approximately 2 hours. A testing approach where the predefined path is considered as representative for all the different situations should therefore take at least 6 consecutive hours.

The test vehicle must be equipped with a Reference Trajectory Measurement System (RTMeS), capable of providing the reference trajectory in any environment with availability 100% and accuracy more than one magnitude better as the positioning terminal being assessed. Generally, the strict accuracy performances of RTMeS require the implementation of high-grade dead reckoning system using geodetic GNSS receiver and high-end antenna coupled with inertial and vehicle sensors with output of at least 10 Hz.

In order to prevent cross masking phenomena, the GBPT antennas on the vehicle's roof should be placed at least 20 cm apart at the roof height up to 2.25 m. When positioned

behind the windshield, the attenuation and masking parameters should be specified.

Additionally, to assess the integrity, the dataset from the GNSS devices under test should provide pseudo-range measurements for each satellite and enable further processing of pseudo-range errors.

These specifications enable the comparison of different test results across the globe to the greatest extent.

C. END-TO-END PERFORMANCE ASSESSMENT

The execution of field tests can deliver valuable information on the behavior of the test set in real environment and serve for calibration purposes of laboratory simulations [60]. When planning the performance assessment methodology, the number of collected samples plays an important role. For example, if the acceptable false detection rate of the Road User Charging (RUC) system had been fixed at 10^{-6} [8], [60] with a confidence level of 95%, approximately $3{*}10^6$ successful tests have to be assessed (Fig. 7). In similar, a field test for the integrity assessment with same requirements at 1 Hz data sampling would take $3{*}10^6$ seconds or 34.3 full continuous days of recording. This is not feasible in real life and should be performed in the scope of laboratory.

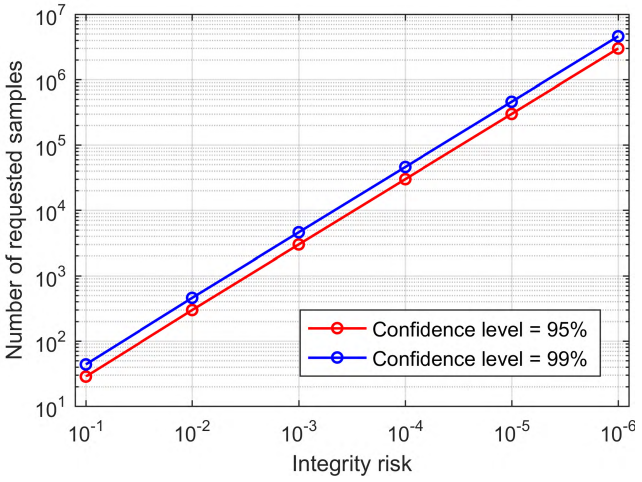

FIGURE 7. Number of required measurement samples for integrity assessment with risk set at the confidence levels 95% (in red) and 99% (in blue).

An overview of *field tests* and *simulations* usage is given in [17], outlining the field validation issues, e.g., non-repeatable satellite signals and constellations (variations over time, upgrading with new satellite generations), changing nature of real environment (foliage, weather, construction works, changed landscape), labor intensive efforts (driver and operator), dedicated certified measurement equipment (reference trajectory, additional sensors), and more. In [60], the necessity for both approaches is expressed in an complimentary manner. The addition of *Record-and-Replay* performance assessment using SDR technology is evaluated in [61], where the *recording* follows the field testing procedures and *replay* the laboratory activities.

Comparing all methodologies, there is a major difference in repeatability, realism, possible duration, execution costs, and inclusion of hybrid positioning. Advantages and drawbacks from each individual approach are reported in a summarized Table 6, described in detail by the results of complementary COST Short-Term Scientific Mission (STSM) [61]. The evaluated operational costs and complexity of laboratory tests may vary up to medium due to special equipment requirements, e.g., GNSS signal simulators and anechoic chambers, while the realistic approach might be difficult to simulate, especially for the constrained operational scenarios as the urban canyon.

TABLE 6. Comparison of field, laboratory, and record & replay approaches [61].

Evaluated category	Field tests	Laboratory tests	Record & Replay tests
Operational costs	high	low	medium
Realistic assessment	high	low	high
Complexity	high	low	high
Repeatability	low	high	high
Valid for Hybrid	yes	no	yes

High repeatability of laboratory and record & replay tests requires the generation of simulated degraded PVT data in a given operational scenario. The EN 16803-1 proposes a *sensitivity analysis* method to assess the performance of a road ITS application or the E2E performance of the whole road ITS system. Its general principle in Fig. 8 comprises the following steps [31]:

1) Definition of the operational scenario as a set of described conditions, and of the test protocol, driven by the use cases;

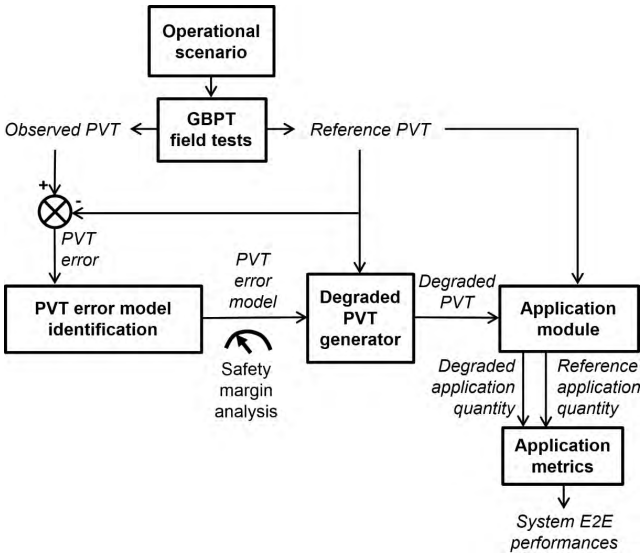

FIGURE 8. Sensitivity analysis principle as presented in EN 16803-1.

2) GBPT field tests execution and data collection for PVT error analyses;
3) PVT error model identification in a form of parametric models with some parameters being random variables;
4) Generation of degraded trajectories with dedicated software using the PVT error model applied to the reference trajectory;
5) E2E performance assessment using the metrics of the system as a function of an error or a deviation with respect to the true value of the quantity;
6) Safety margin analysis as a repeating task with increasing errors until the required E2E performance is no longer satisfied.

IV. MEASUREMENT CAMPAIGN IN NANTES

The measurement campaign for positioning performance assessment of geodetic, automotive, and smartphone GNSS receivers took place in the city of Nantes and its surroundings in western France in September 2016 as a supportive act to the CEN-CENELEC efforts at addressing some scientific issues that required common agreement.

Within the scope of COST Action TU1302 (SaPPART), a 3-week STSM started between University of Ljubljana, Faculty of Electrical Engineering, and the GEOLOC Laboratory at the French Institute of Science and Technology for Transport, Development, and Networks (IFSTTAR) in Nantes. During an experimental data collection campaign across several specific environmental scenarios with multiple grades of GNSS receivers, valuable data have been collected and analyzed. The following sections outline the measurement set-up and operational conditions as the foundation for the final results.

A. MEASUREMENT TRAJECTORIES

The historical Nantes region is known by the river Loare and vineyards landscape, where *Mountainous* and *Modern Urban Canyon* high-level reference environments from European standard EN 16803-1 [31] are not accessible. To maximize the conformity to the rest of 4 categories, the area diversity was studied by IFSTTAR experts in detail and 4 trajectories were finally selected.

The first trajectory was following the peripheral ring road, placed around the city of Nantes (Fig. 9a). it includes tall bridges across the river Loare, several overpasses, junctions, and recessed lanes under the surrounding levels.

The second trajectory was placed on the highway sections from Nantes over Angers and Cholet back to the origin (Fig. 9b). The route leads across flat countryside with many overpasses, lower masking angles, and some recessed driving lanes. There is a tunnel of approximate length 1700 m on the section A11 Avrillé-Angers.

The third trajectory led across the Nantes urban center north from the island (Fig. 9c). The city center does not contain many modern skyscrapers with high masking angles, therefore the condition was met mostly for the European Urban scenario. An exact urban route could not be followed

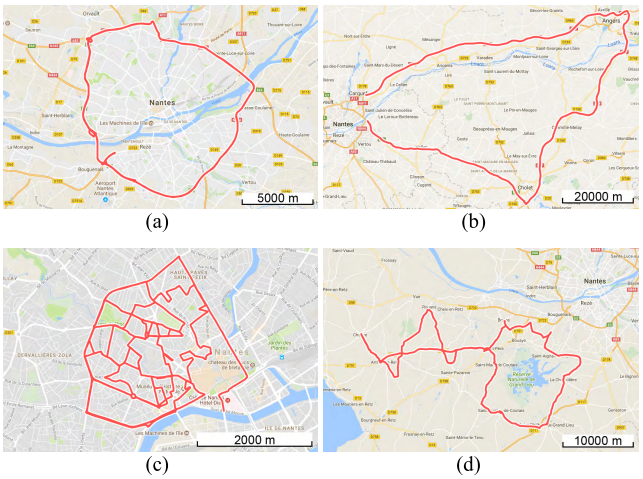

FIGURE 9. Visualization of measurement trajectories - (a) Nantes Peripheral Ring Road, (b) Highway Nantes-Angers-Cholet, (c) Inner Urban City of Nantes, and (d) Nantes Rural.

in all 3 runs due to roadworks that changed during the day, but those minor deviations should not have a significant impact on the statistics.

The fourth and last scenario was placed on the countryside roads west from Nantes towards the Ocean (Fig. 9d). This route mostly conforms the Tree-lined Rural reference environment with small additions of Flat Rural and European Peri-urban.

The characteristics of all trajectories are summarized in Table 7 with merged lengths and durations of 3 daily runs.

TABLE 7. Characteristics of measurement trajectories.

Day	Measurement trajectory name	Reference environment name	Date of test	Trajectory length and duration
1	Nantes Peripheral Ring Road	European Peri-Urban	21.09.2016	358.0 km / 5.12 h
2	Highway Nantes-Angers-Cholet	Flat Rural	22.09.2016	613.0 km / 5.71 h
3	Inner Urban City of Nantes	European Urban	26.09.2016	121.5 km / 6.78 h
4	Nantes Rural	Tree-lined Rural	27.09.2016	333.3 km / 6.49 h

B. GNSS RECEIVERS UNDER TEST

GNSS receivers, used during the measurement campaign, were divided into 3 main groups according to receiver type, expected performance, antenna position, and typical use case:

Group 1: geodetic receivers with post-processing (PPK) ability and professional antennas (abbreviated as GR);

Group 2: low-cost receivers in automotive mode with patch antenna on the roof of the vehicle (abbreviated as AR);

Group 3: various brands of smartphones and a mobile Bluetooth receiver placed behind the windshield inside the vehicle (abbreviated as SR).

The characteristics of all receivers are presented in Table 8, including their short names, e.g., SR2 is the second member

TABLE 8. The characteristics of GNSS receivers under test.

ID	Short Name	Manufacturer and Model or Chipset	Rate (Hz)	Constellation used	NMEA Output	RAW Output	PPK Used	Sensor data	Android version
1	GR1	Novatel DL-V3	10	GPS + GLONASS	No	Yes	Yes	No	n/a
2	GR2	Septentrio AsteRX3	10	GPS + GLONASS	No	Yes	Yes	No	n/a
3	GR3	Septentrio AsteRX3	1	GPS + SBAS	Yes	No	No	No	n/a
4	AR1	uBlox NEO-M8N	1	GPS + GLONASS + SBAS	Yes	Yes	No	No	n/a
5	AR2	uBlox NEO-M8N	5	GPS + SBAS	Yes	No	No	No	n/a
6	AR3	uBlox NEO-M8T	1	GPS + GLONASS + SBAS	Yes	Yes	No	No	n/a
7	AR4	uBlox NEO-M8U	1	GPS + GLONASS + SBAS	Yes	Yes	No	Yes	n/a
8	AR5	uBlox LEA-6T	5	GPS + SBAS	Yes	Yes	No	No	n/a
9	AR6	uBlox LEA-5H	1	GPS only	Yes	No	No	No	n/a
10	AR7	uBlox LEA-4T	1	GPS only	Yes	No	No	No	n/a
11	AR8	SiRF IV BU-353	1	GPS only	Yes	No	No	No	n/a
12	SR1	Huawei P8	1	GPS + GLONASS	Yes	No	No	No	5.0.1
13	SR2	Samsung Note 4	1	GPS + GLONASS	Yes	No	No	No	5.1.1
14	SR3	Samsung S4 mini	1	GPS + GLONASS	Yes	No	No	Yes	4.4.2
15	SR4	Acer Liquid Jade	1	GPS + GLONASS	Yes	No	No	No	4.4.4
16	SR5	Wiko Fever	1	GPS + GLONASS	Yes	No	No	No	5.1
17	SR6	HTC One mini	1	GPS + GLONASS	Yes	No	No	Yes	4.4.2
18	SR7	Wintec WBT-202G	1	GPS + SBAS	Yes	No	No	No	n/a

of the smartphones group. Note, that GR2 and GR3 are physically one receiver providing two different outputs.

1) GEODETIC RECEIVERS

Geodetic receivers are professional devices, used for mapping or for surveying positions where up to several cm of precision are needed. To achieve best results, they require the use of real-time or post-processing algorithms, connection to a larger multipath rejection antenna (Fig. 10), and clear sky visibility in order to preserve phase measurement continuity and avoid cycle-slips. Due to these restrictions and higher equipment price geodetic receivers cannot be found in mass-market ITS services today, still their excellent positioning performance is needed in most demanding services. In our analyses the performance of two geodetic receivers is assessed: GR1 and GR2/GR3.

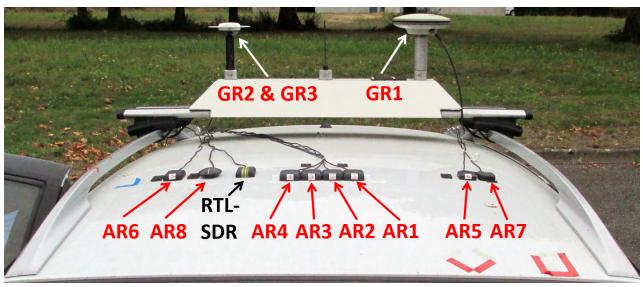

FIGURE 10. Placement of geodetic and automotive receivers' antennas on top of VERT.

The GR2/GR3 is a multi-constellation (GPS, GLONASS, and GALILEO) and multi-frequency (L1, L2, L5, E5a, E5b, E5 AltBOC) code/carrier tracking receiver, connected to a G5Ant-52AT1 antenna. It provides raw measurements up to 100 Hz and NMEA v2.30 output format, up to 10 Hz. Its position accuracy is estimated at 1.3 m horizontal (1-sigma) in standalone mode and 0.6 cm + 0.5 ppm in RTK performance [62]. Two streams of data from this receiver were recorded: raw data for post-processing and a standalone solution providing NMEA (only GGA and ZDA sentences, no GSA and GSV satellite status).

The GR1 receiver features GPS and GLONASS functionality using the NOV702GGL antenna with additional capability of tracking GPS L2C and L5. It provides raw measurements up to 50 Hz with horizontal accuracy up to 1 cm + 1 ppm RMS (RT-2) [63]. No standalone solution was provided, only the raw data for the post-processing. This receiver is an integral part of the RTMeS and GNSS errors may have penetrated to the RTMeS output, therefore the performance assessment in the final results might be biased. It was still decided to keep this receiver as one of the test receivers.

2) AUTOMOTIVE ROOF-MOUNTED ANTENNA RECEIVERS

The second group of receivers is based on multiple low-cost GNSS receivers from different chipset manufacturers. They provided single- and multi-constellation abilities, NMEA datasets, proprietary binary outputs, and the support for Satellite-Based Augmentation Systems (SBAS, EGNOS). The characterization as *automotive* resides from the settings of uBlox receivers for dynamic platform models [35], adjusting the navigation engine to the expected application environment. The *Automotive* model suits well for applications with equivalent dynamics to those of a passenger car with low vertical acceleration assumed.

Some receivers provide special features, e.g., the AR1 with firmware FW2.01 supports additional undocumented binary packets TRK-MEAS and TRK-SRFBX, providing partial capability for post-processing (recorded only for experimental future work), and the AR4 introduces untethered dead reckoning (UDR) technology with onboard accelerometer and gyroscope [56]. The AR8 USB receiver provides the satellites-in-view (GSV) information only every 5 seconds,

limiting certain constellation analyses. The summary of their characteristics is summarized in Table 8.

The mounting and placement of geodetic and automotive antennas is presented in Fig. 10. Antennas from geodetic receivers are positioned apart with respect to the field test design specifications from EN 16803-1 [31] due to their larger design and permanent mounting on the measurement vehicle. Some receivers' antennas are positioned in clusters in order to simplify the transformation and processing of multiple reference trajectories (Table 9).

3) SMARTPHONES AND IN-VEHICLE ANTENNA RECEIVERS

The third group consists of handheld devices with embedded GNSS antenna primarily to be used inside the vehicle. Their placement behind the windshield is presented in Fig. 11. All but one are Android smartphones of different generations (2013 onwards) with different chipsets, single- or multi-constellation abilities, various on-board sensors, and version of Android OS. The only left is a mass-market Bluetooth GPS receiver SR7 with the GNSS core comparable to AR6 from the automotive group, having the patch antenna inside the module. The antenna micro location inside the devices was not studied since displacement is considered to be much smaller than the average positioning error. All receivers from SR group provided data in NMEA format at 1 Hz rate. The summary of their characteristics is presented in Table 8.

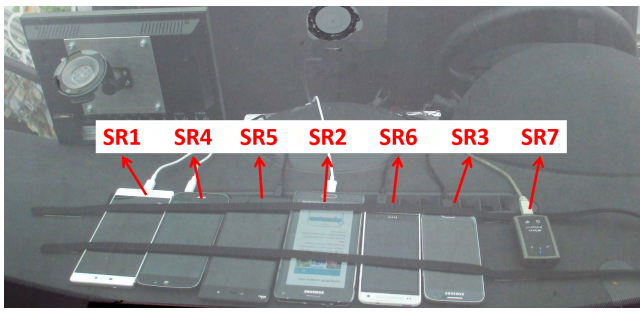

FIGURE 11. Placement of smartphones and Bluetooth receiver module behind the windshield.

NMEA recording on the devices was realized by an Android application NMEA Recorder (by Thomas Wolf). Smartphone sensor data were also recorded for the future use by the application AndroSensor (by Fiv Asim). WinTec module had Bluetooth connection to Samsung S4 mini, where the data was stored in real-time by application BlueTerm (by pymasde.es).

C. THE REFERENCE TRAJECTORY MEASUREMENT SYSTEM AND THE EXPERIMENTAL VEHICLE

An accurate position reference is needed to assess the errors in spatial accuracy. To ensure proper detection of small differences in PVT, the reference performance must outstand the test receivers by at least a magnitude.

The RTMeS used during the field tests is an integral part of the IFSTTAR's instrumented Vehicle for Experimental Research on Trajectories (VERT) [64], established to support research activities by assuring the precise vehicle trajectory. The GEOLOC laboratory at IFSTTAR decided for the adaptation of Renault Clio III Grandtour to allow simple attachments of additional measurement equipment to the interior or exterior while still being able to cruise the narrow urban streets. It features an auxiliary battery-powered supply unit, powerful computer with i7 cores for recording and real-rime processing purposes, and two displays for the operators on the front and rear passenger seats [64].

The core element of the RTMeS architecture (Fig. 12) is the Inertial Navigation System (INS), which performs real-time coupling of data from a 3-axis fiber optic gyroscope, a 3-axis accelerometer, an odometer attached to rear wheels, and a dual-frequency GNSS receiver GR1. The estimated accuracies with full GNSS support are 0.01° RMS estimates of the roll, pitch, and yaw angle, 3.5 cm in the horizontal plane, and 5 cm along the vertical axis [64].

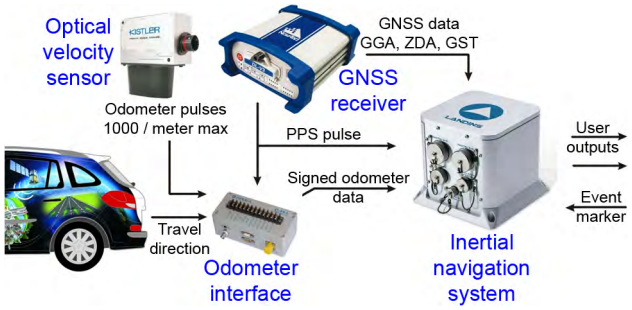

FIGURE 12. The architecture of RTMeS inside the vehicle VERT [64].

The RTMeS provides an accurate initial reference trajectory for one specific point inside the INS unit. Since the antennas from devices are spatially distributed on the vehicle's top and behind the windshield, the differences in their navigation solution and the initial reference can reflect a larger error in position or velocity. To avoid these biases, the positions of antennas were measured relatively to known markings of the vehicle in order to establish lever arms for the transformations from the INS to the antennas' phase centers. Finally, a total of 7 additional reference trajectories (RT) were computed using these data by the software package PopINS from IXSEA [64]. The Table 9 summarizes their characteristics.

TABLE 9. Reference trajectories for clusters of receivers.

Ref. name	GNSS receivers	Cluster	Relative position	Spatial reference	Estimated error
RT1	GR1	No	Known	GR1	0 cm
RT2	GR2-GR3	No	Known	GR2/GR3	0 cm
RT3	AR1-AR4	Yes	Measured	Mid-point	Up to 8 cm
RT4	AR6, AR8	Yes	Combined	AR6	0 cm / 16.5 cm
RT5	AR5, AR7	Yes	Combined	AR5	0 cm / 5 cm
RT6	SR1-SR6	Yes	Measured	Mid-point	Up to 20 cm
RT7	SR7	No	Measured	SR7	0 cm

Clustering of antennas has been used to reduce the number of RTs, to save storage space, processing memory and power during the analyses. A single cluster containing several devices uses only one lever arm, so the error increases towards the outer device, e.g., in smartphones case with the reference set to the mid-point between 3rd and 4th device. The error estimation in Table 9 is based on the device dimensions and its relative position to the nearest known marking, where GR1, GR2/GR3, AR5, AR6, and AR7 completely align with the known markings. In this case an error-free estimation is assumed, although the actual position of antenna phase center inside the antennas, smartphones, and modules was not studied in detail. According to Fig. 10 and Fig. 11 most of the estimated error is in lateral or cross-track direction.

V. EXPERIMENTAL RESULTS

This section outlines the results of our analyses with the most important impact in road ITS applications. Where possible, the analyses were performed with respect to the standard EN 16803-1 [31] and the COST Action SaPPART [33].

After field test data collection, all the recordings were checked for the epoch availability, checksum validity, timestamps continuity, and conformance to the initial settings. The verification of data and final analyses were executed using programming scripts in Python 2.7 and Matlab 2016a.

In theory, using 18 data streams from 17 receivers across 4 scenarios with 3 daily runs would provide 216 individual datasets. After the verification phase only 196 or 90.7% of them were kept for further processing and declared as valid. The remaining 9.3% belong to complete data removal of the damaged SR6 with low GNSS signal levels and much degraded performance, missing tracks from smartphones SR5 and SR2 that suffered from going into deep sleep and pausing the data recording, and minor data loss at GR2/GR3 and AR7 receivers due to temporary infrastructural power delivery failure.

A. HORIZONTAL ACCURACY

The assessment of position accuracy across all the receivers and environments using an accurate RTMeS was an important goal of our measurement campaign. The groups of receivers from Table 8 were expected to belong to distinct accuracy classes, e.g., geodetic to Class 1, automotive with roof-mounted antenna to Class 2, and smartphones to Class 3 for the clear-sky scenarios.

Data collection procedures followed the field test guidelines, therefore each trajectory was tested 3-times daily with time spacing of at least 2 hours. To avoid biased data for stationery measurements, the epochs with speed below 2 km/h were excluded from further accuracy processing. With help of the 7 computed reference trajectories from Table 9, the Horizontal Position Error (HPE) was derived and assessed. The results in a form of Cumulative Distribution Function (CDF) for highway and deep urban environmental scenarios are presented in Fig. 13.

The solid curves on the left belong to geodetic receivers GR1 and GR2/GR3, with the latter shown in post-processing (GR2) and standalone mode (GR3). The GR1 performance might be biased since it is also invoked in the reference trajectory computation process. From the clear-sky perspective (Fig. 13a), next best results come from the latest generation automotive receivers with roof-mounted antennas (AR1-AR4), followed by dashboard Bluetooth module SR7 and some of the smartphones. The remainder belongs to the mixture of older generation automotive receivers with external antenna and smartphones.

In more obstructed urban scenario (Fig. 13b), the geodetic receivers using PPK behave similar to the clear-sky scenario up to the 75th percentile, followed by the mixture of latest generation automotive receivers and some smartphones. Surprisingly, the standalone geodetic receiver GR3 with professional antenna provides good results only up to the 50th percentile, afterwards the CDF gets flatter and at 95% reaches 6.29 m error margin, 2.67 m after the automotive AR1 with roof patch antenna. The worst group of 4 receivers (SR1, SR4, SR5, and older AR7) crosses the 95% mark from 10.25 m to 16.36 m. The AR5 curve is somehow biased in a cross-track direction for unknown reasons, that couldn't be estimated fairly even after additional examination.

The Nantes ring peripheral and rural scenarios behave similar to highway with some minor shuffling of receivers order, because the highway is also slightly obstructed by 120 overpasses, recessed driving lanes, and additional foliage.

B. ALONG-TRACK AND CROSS-TRACK ACCURACY

Along-track and cross-track accuracy assessments are based on the position and heading of the reference trajectory. Along direction is the vector of movement, e.g., towards the road section ahead, and cross direction is the lateral vector, being perpendicular to the heading. The cross-track error is in some literature referred to as off-track error [37], [65].

In our analysis the Along-Track Error (ATE) has negative sign if the location from the test receiver is somewhere behind the vehicle or at least in the direction towards back of the vehicle. The Cross-Track Error (CTE) gets negative sign if the reported position is left from the direction of driving, and positive for being reported right from the vehicle. The analysis was performed on the same dataset as HPE with decomposition of HPE value to its directional components as depicted in [65].

Firstly the distribution of ATE and CTE around the reference positions was analyzed. The ATE distribution for automotive receivers is centered on the interval $[-1, 0]$ m and quite symmetrical, while the smartphones reflect the similar symmetry only for the highway scenario (Fig. 14a). The urban environment for the smartphones causes a heavy tail down to -15 m behind the vehicle (Fig. 14b). For the urban scenario also the distribution center in spread on the interval $[-4, -1]$ m, similar to the antenna location effect study in [55].

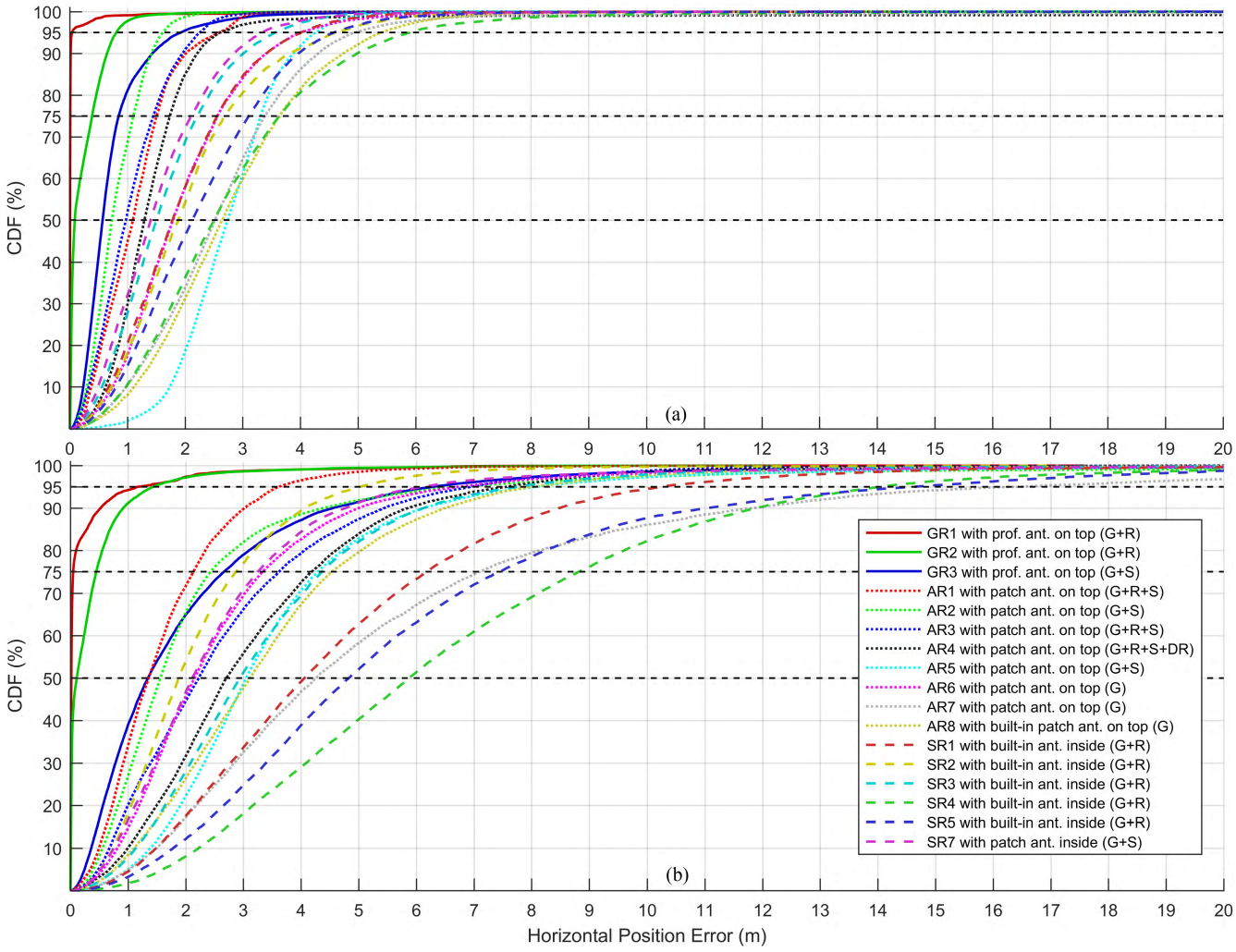

FIGURE 13. The Cumulative Distribution Function (CDF) of Horizontal Position Errors (HPE) for (a) Highway Nantes-Angers-Cholet and (b) Inner Urban City of Nantes. The GNSS constellations scheme is: G for GPS, R for GLONASS, S for EGNOS as SBAS, and DR for integrated sensor fusion. The 3 horizontal dashed lines represent the set of three statistical values given by the 50th, 75th, and 95th percentiles of CDF.

The CTE for any receiver group is symmetrically distributed around the interval $[-1, 0]$ m, centered slightly left from the vehicle in the driving direction. The distribution is long-tailed for urban scenario in both directions up to 7 m (95%) for the automotive receivers and up to 10 m (95%) for the smartphones.

The overview of ATE, CTE, and combined HPE performance for all the receivers in highway and urban environments is presented in Fig. 15 in a form of grouped and stacked bars. This form is very suitable to check the receiver compliance with possible classification limits e.g. the services that require improved directional accuracy, are intelligent speed adaptation and autonomous cruise control (ATE), and lane departure and warning systems (CTE) [37].

C. POSITION AVAILABILITY

The availability is defined in terms of the likelihood that accuracy, continuity and integrity parameters meet the requirements of the target application [66]. This paper follows the definition from the standard [31] for the position availability as the percentage of time intervals of length T during which the positioning terminal provides at least one position output.

To cover specific needs of various applications the availability interval T was selected as 0.2 s, 0.5 s, 1 s, 2 s, 5 s, 10 s, 30 s, and 60 s. Although the requirement of 0.2 s (5 Hz) is very strict, it was still tested because 2 receivers provided 5 Hz output with some jittering, that lowers the overall performance in 0.2 s interval (Fig. 16). The highest availability belongs to the rural scenario at 73.1% and 73.2% for AR2 and AR5, and lowest to the urban scenario at 70.4% and 70.6%. To avoid unnecessary loss of availability for the highway scenario with tunnel of approximate length 1700 m, this observation interval was removed from all the availability analyses.

The results for all the receivers using $T = 1$ s are summarized in Table 10. The lowest availability is provided by geodetic receivers and the oldest receiver AR7. The average

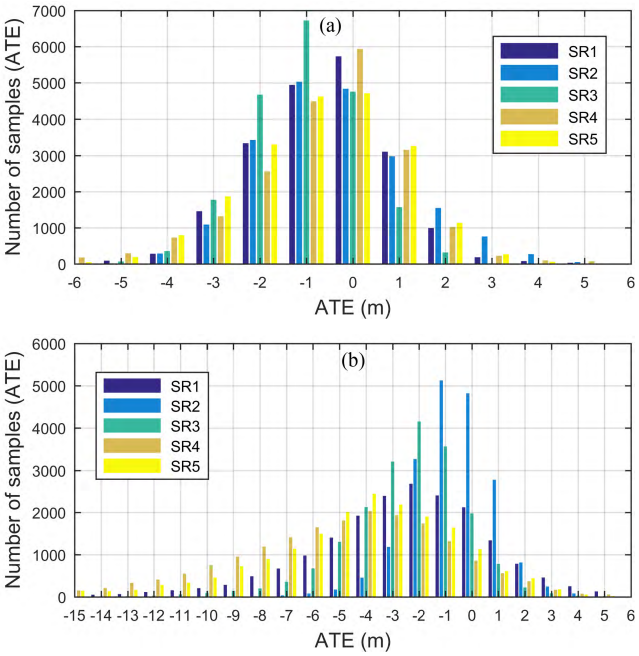

FIGURE 14. Along-track error distribution for smartphones (a) on the highway and (b) in urban scenario.

percentage across all 4 scenarios for geodetic receivers is 96.416% with minimum of 87.182% for the GR1. While the results for latest generation of automotive 1 Hz receivers

TABLE 10. T-availability (T = 1 s) with percentage of time during which the output of the positioning terminal is available,

GNSS Receiver	Availability Ring (%)	Availability Highway (%)	Availability Urban (%)	Availability Rural (%)
GR1	87.182	90.814	87.960	95.197
GR2	98.670	99.808	99.537	99.943
GR3	98.637	99.813	99.451	99.975
AR1	100	100	100	100
AR2	99.788	99.970	99.742	99.893
AR3	100	100	100	100
AR4	100	100	100	100
AR5	100	100	99.885	99.974
AR6	100	100	100	100
AR7	97.953	99.533	95.950	99.573
AR8	99.989	99.995	100	100
SR1	99.957	100	100	99.996
SR2	100	100	100	100
SR3	100	100	100	100
SR4	100	100	100	100
SR5	100	99.995	100	99.996
SR7	100	99.995	100	99.996

AR1, AR3, and AR4 always reach 100%, the INS supported AR4 is the only one that provides 100% also with the tunnel included. The accuracy results for AR4 are still not encouraging since the untethered support shows many glitches, e.g., inside the last third of the tunnel, where the reported position suddenly slows down and virtually stops, still providing valid output for 34 s with INS only flag marked. The 5 Hz receivers

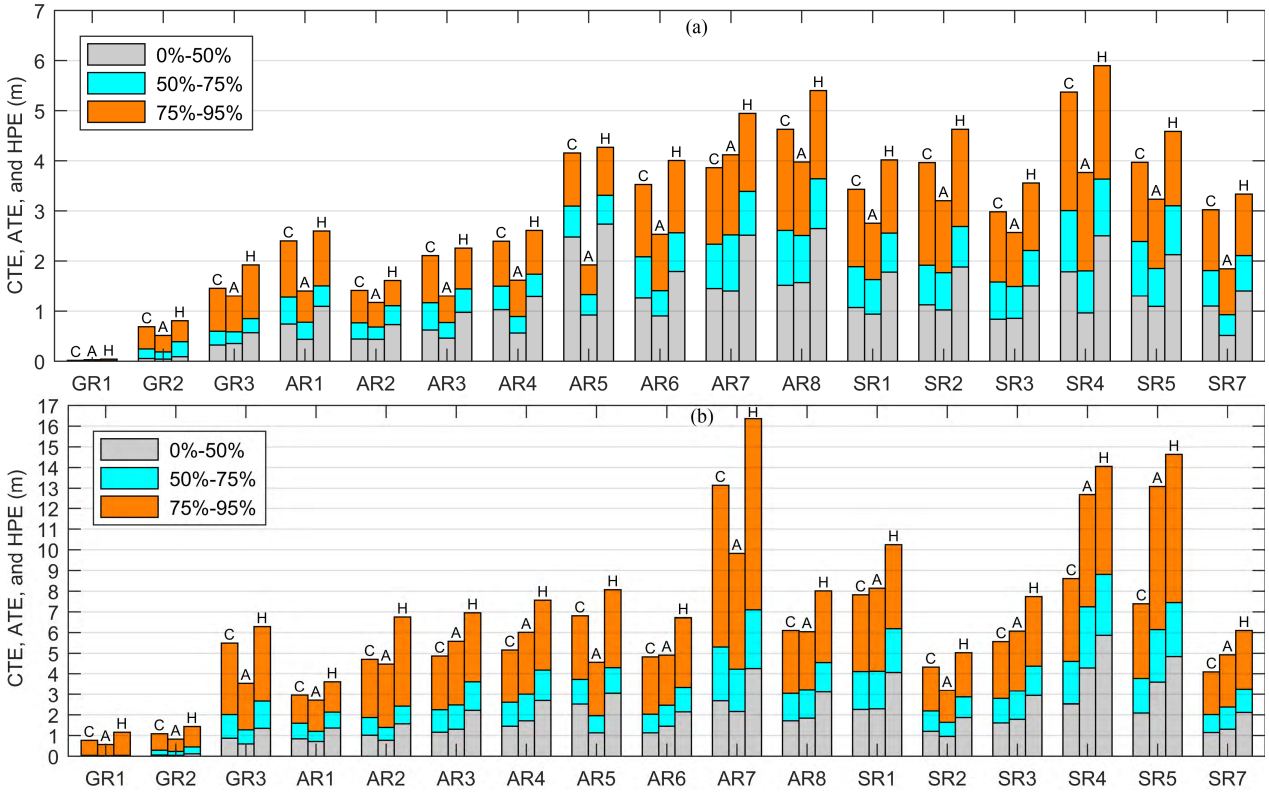

FIGURE 15. The presentation of Cross-track (C), Along-track (A), and Horizontal Position Error (H) for (a) Highway Nantes-Angers-Cholet and (b) Inner Urban City of Nantes. The tri-colored bars represent the bottom-up set of three statistical values given by the 50th (start of cyan bar), 75th (start of orange bar), and 95th (end of orange bar) percentiles of CDF.

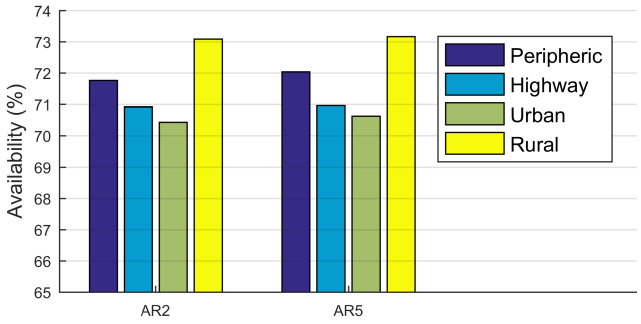

FIGURE 16. Availability of 5 Hz receivers across all 4 scenarios.

also showed some lack of position fixes and the initial consistency check report confirms it is mostly for the transmission and recording problems of 5 Hz data stream. Also the smartphones should respond with highest availability, but due to occasional problems with storing the data in the internal memory (e.g., missing a part of the epoch) the average is 99.997% with minimum received from SR1. Only the urban scenario reached 100% here without any interruptions, therefore confirming high availability and lower accuracy for the smartphones.

The results for $T = 10$ s are available in Table 11 and showing only receivers with less than 100% availability. Ten seconds interval filters out any small glitches, jittering, and data recording problems, so only most vulnerable receivers are shown. The geodetic receiver GR1 reaches only 96.396% in urban scenario, because after losing a position fix the recovery lasted up to several tenths of seconds.

TABLE 11. T-availability (T = 10 s) with percentage of time during which the output of the positioning terminal is available.

GNSS Receiver	Availability Ring (%)	Availability Highway (%)	Availability Urban (%)	Availability Rural (%)
GR1	99.620	99.852	96.396	98.802
GR2	100	100	99.959	100
GR3	100	100	99.959	100
AR7	99.620	99.902	98.809	100

The $T = 30$ s interval for GR1 gives 99.265% for the urban, and 99.872% for the rural environment. For the urban scenario the GR2/GR3 reaches 99.959% and the oldest AR7 only 99.437%. All others provide 100%, as well as for the availability interval set to $T = 60$ s, where all tested candidates provided full availability.

D. AVAILABILITY DISTRIBUTION

The global availability results from Tables 10 and 11 provide the statistical evaluation over the whole measurement duration. By this, the information of how these events with no position fix are distributed over time, is removed. Considering the application where 1 s losses of PVT solution are tolerated without degradation, and 5 s loss might fail the E2E requirements, this information would reveal important risks. The examples for such approach include most of the navigation applications and parking per minute basis [31].

Fig. 17 presents the distribution analysis for the urban environment for the receivers in Table 10 with position availability $T = 1$ s less than 100%. The stacked bars are grouped per interval basis, e.g., all consecutive missing epochs from 1 to 5 seconds are shown as the lower bin. This figure proves that GR1 reaches low global availability in Table 10 due to 72.49% share of the bin, where 11 or more consecutive seconds are missing. Most receivers provide shorter outages of up to 10 seconds. The number n above the bars shows the count of all intervals with 1 or more position loss as a basis for the bins ratios.

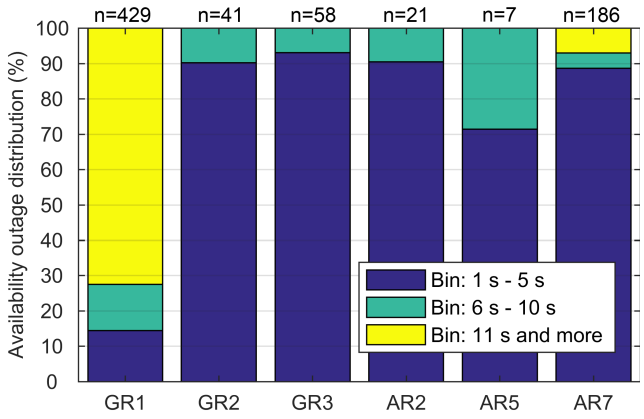

FIGURE 17. Availability outage distribution for the urban environment.

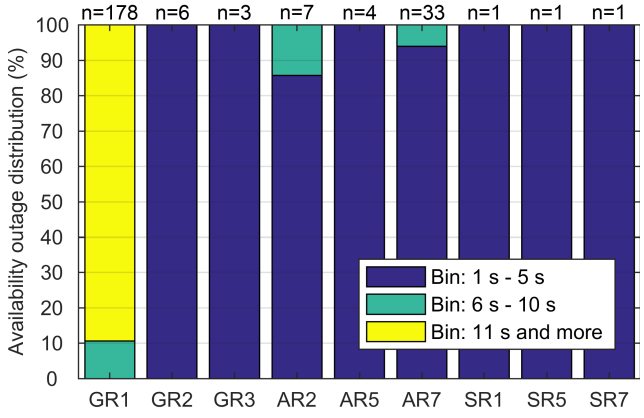

FIGURE 18. Availability outage distribution for the rural environment.

Fig. 18 includes the receivers with missing epochs for the rural scenario from Table 10. Most of outages occur in duration less than 6 seconds with only exception at GR1, having 89.33% of losses in the upper bin.

VI. CLASSIFICATION OF ACCURACY AND AVAILABILITY

This section provides classification aspects of accuracy and availability with definition of performance classes from multiple sources, merged in SaPPART Guidelines [33]. When assessing the GNSS performance, at least two approaches can

be considered: from the GNSS technology perspective and from the application requirements.

A. CLASSIFICATION OF ACCURACY

Starting from our measurement campaign, Fig. 13 presents the accuracy performance results in a form of cumulative probability of horizontal error (CDF). The preliminary hypothesis among the SaPPART group was the existence of virtual limits between the 3 different groups of receivers, with placeholders seen as gaps in CDF plot.

In Fig. 13 two larger and several smaller gaps can be seen, especially for the urban scenario, where GR2 crosses 50-75-95 percentile boundaries at 0.11-0.45-1.43 m. After the first gap, other receivers continue at 1.35-2.13-3.62 m, providing the blank space with lengths of 1.24-1.68-2.19 m at percentiles triplet. The next larger gap in urban scenario is from AR8 at 3.12-4.54-8.01 m to SR1 at 4.06-6.18-10.25 m.

From this scenario it is obvious that receivers from different groups belong to the same technology class, where class is defined as the group of receivers with similar performances. The first class here contains only PPK receivers, the second merges a mix of latest generation automotive receivers AR1-AR4, geodetic GR3 in standalone mode, and better smartphones, and the third one embraces the worst performance smartphones and the oldest receiver AR7.

Based on these results, the receiver groups GR, AR, and SR were divided into 2 subgroups according to their specifics. The first subgroups from previous groups, e.g., SG11, SG21, and SG31 in Fig. 19, comprise devices with better performance, while the second subgroup, e.g., SG12, SG22, and SG32, contains the rest. For the urban scenario the preselected dataset is the following: SG11 (GR1, GR2), SG12 (GR3), SG21 (AR1-AR4), SG22 (AR5-AR7), SG31 (SR1-SR3), and SG32 (SR4, SR5).

In the case of urban scenario, these subgroups almost perfectly coincide and provide a starting point that can lead to the classification as presented in Fig. 5 for P50, P75, and P95 percentiles. Since most of the road ITS systems are deployed in mixed environments, there should be a unified classification procedure across all of them.

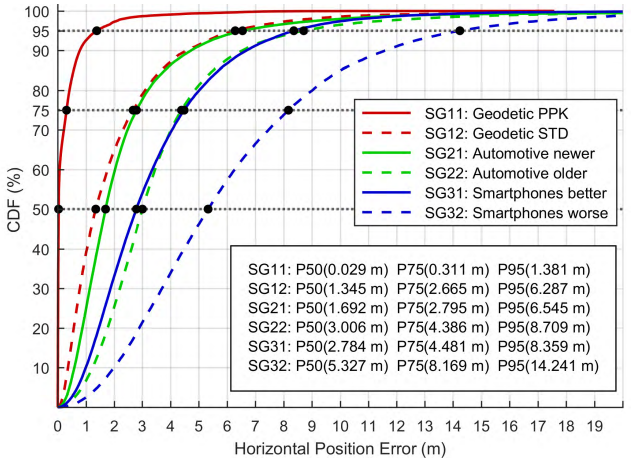

FIGURE 19. Subgrouping of GNSS receivers from urban environment and the corresponding CDF for subgrouped HPE.

The classification results for all the receivers based on Table 3 boundaries are summarized in Table 12. The classes for each environment in columns 2 to 5 are chosen from the percentile boundaries as the maximum class from any percentile. The decision for the final class is based again on the worst parameter in a row, i.e. the maximum value from all 4 environments.

TABLE 12. Horizontal accuracy performance classification - the technology perspective.

GNSS Receiver	Class Ring	Class Highway	Class Urban	Class Rural	Mean Value	Max Class
GR1	1	1	2	1	**1.25**	**2**
GR2	2	2	2	1	**1.75**	**2**
GR3	2	2	3	2	**2.25**	**3**
AR1	2	2	2	2	**2.00**	**2**
AR2	2	2	3	2	**2.25**	**3**
AR3	2	2	3	2	**2.25**	**3**
AR4	2	2	3	2	**2.25**	**3**
AR5	3	3	3	3	**3.00**	**3**
AR6	2	2	3	2	**2.25**	**3**
AR7	3	3	3	3	**3.00**	**3**
AR8	3	3	3	3	**3.00**	**3**
SR1	3	2	3	3	**2.75**	**3**
SR2	3	2	3	2	**2.50**	**3**
SR3	2	2	3	2	**2.25**	**3**
SR4	3	3	3	3	**3.00**	**3**
SR5	3	3	3	3	**3.00**	**3**
SR7	2	2	3	2	**2.25**	**3**

An interesting and new visual approach can be seen in Fig. 20 presenting only the 95th percentile marks from Table 3 for all the receivers in all 4 environments. Using this visualization it is easy to detect the horizontal accuracy characteristics of each receiver in any environment.

The second type of classification is based on Table 4, presenting the requirements of various road applications. The classification results in Table 13 are not encouraging for

TABLE 13. Horizontal accuracy performance classification - the applications perspective.

GNSS Receiver	Class Ring	Class Highway	Class Urban	Class Rural	Mean Value	Max Class	Max Name
GR1	1	1	3	1	**1.50**	**3**	Carriageway
GR2	2	2	3	2	**2.25**	**3**	Carriageway
GR3	3	3	3	3	**3.00**	**3**	Carriageway
AR1	3	3	3	3	**3.00**	**3**	Carriageway
AR2	3	3	3	3	**3.00**	**3**	Carriageway
AR3	3	3	3	3	**3.00**	**3**	Carriageway
AR4	3	3	3	3	**3.00**	**3**	Carriageway
AR5	3	3	3	3	**3.00**	**3**	Carriageway
AR6	3	3	3	3	**3.00**	**3**	Carriageway
AR7	3	3	4	3	**3.25**	**4**	Area
AR8	3	3	3	3	**3.00**	**3**	Carriageway
SR1	3	3	4	3	**3.25**	**4**	Area
SR2	3	3	3	3	**3.00**	**3**	Carriageway
SR3	3	3	3	3	**3.00**	**3**	Carriageway
SR4	3	3	4	3	**3.25**	**4**	Area
SR5	3	3	4	3	**3.25**	**4**	Area
SR7	3	3	3	3	**3.00**	**3**	Carriageway

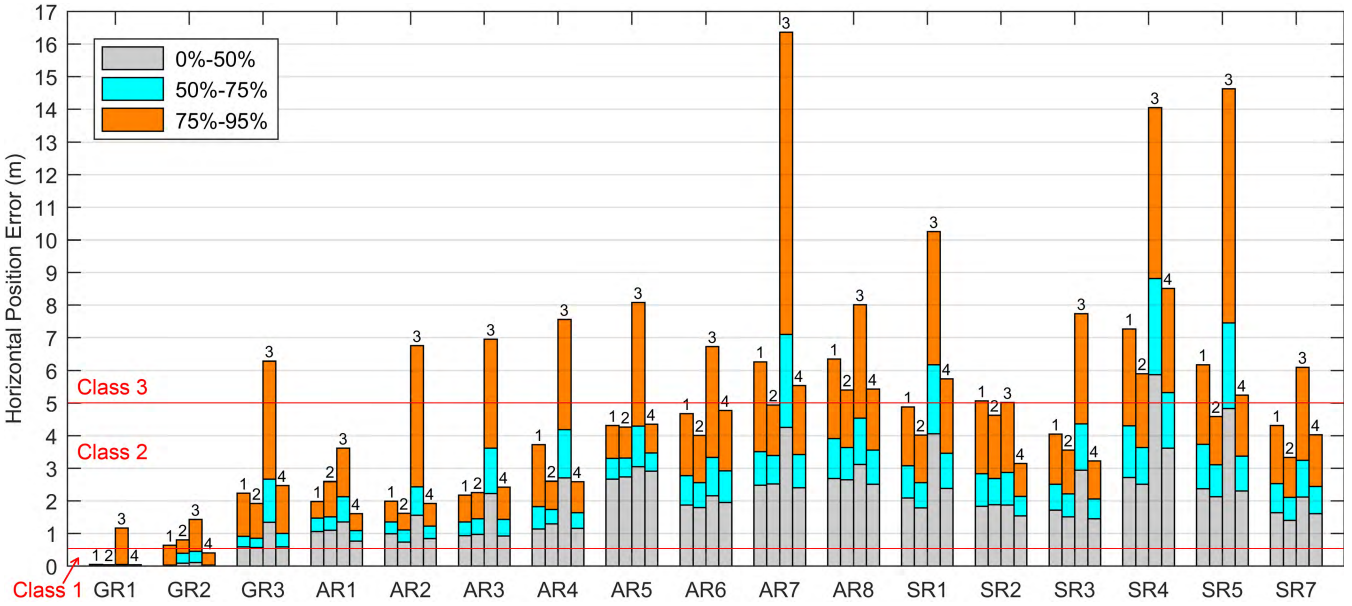

FIGURE 20. The presentation of Horizontal Position Error (HPE) for 4 reference environments: (1) Nantes Peripheral Ring, (2) Highway Nantes-Angers-Cholet, (3) Inner Urban City of Nantes, and (4) Nantes Rural. The tri-colored bars represent the bottom-up set of three statistical values given by the 50th (start of cyan bar), 75th (start of orange bar), and 95th (end of orange bar) percentiles of CDF. Class boundaries for 95th percentile from Table 3 are presented as horizontal red lines.

high demands since the classes in urban environment start at carriageway, omitting sub-meter accuracy at 95% CDF. On the contrary, GR1 is classified with best In-lane accuracy in all other environments, as well as GR2, providing Lane accuracies.

This is the reason, why standard EN 16803-1 [31] introduces the weighted mean of the performances measured individually in different reference environments. Tables 12 and 13 contain the mean class field using equal weights.

B. CLASSIFICATION OF AVAILABILITY

The classification of availability is based on data from Table 10 with availability interval set to 1 s. Class boundaries are provided in Table 5, using 95% and 99% limits. The summarized results are available in Table 14.

The majority of receivers in Table 10 satisfy the 99% availability requirement across all the environments. The oldest AR7 is the only outlier from the automotive group with roof antenna providing the result below the 99% limit for the ring and urban scenarios. The outage distribution for the urban environment in Fig. 17 shows that from total of 186 outage gaps, 8 belong to the 6-10 s bin, and 13 to the 11 s and more bin, significantly reducing the overall availability. The geodetic receivers, especially GR1, suffer from slow position fix recovery causing major outages, e.g., from total of 429 events 311 or 72.5% belong to the upper bin.

C. DISCUSSION

The horizontal accuracy assessment presents the performance diversity of the receiver groups, e.g., automotive receivers with antenna on the top of the vehicle, where the latest generation receivers perform much better than the older ones. There are also similarities in accuracy between the receivers from different groups, e.g. newer multi-constellation smartphones placed inside the vehicle closely follow the best automotive receivers with roof antenna.

The described group overlapping can be noticed through the intersecting CDF curves in Fig. 13a. This fact prevents us from setting the unambiguous limits for the classification of receivers from the technology perspective. The statistical subgrouping in Fig. 19 provides larger gaps between the subgroups, resulting in conformance to the 50th and the 75th percentile boundaries in Table 3. From the cross- and along-track analyses in Fig. 15 it can be established that CTE

TABLE 14. Horizontal availability performance classification for T = 1 s as proposed by COST Action SaPPART.

GNSS Receiver	Class Ring	Class Highway	Class Urban	Class Rural	Mean Value	Final Class
GR1	3	3	3	2	**2.75**	**3**
GR2	2	1	1	1	**1.25**	**2**
GR3	2	1	1	1	**1.25**	**2**
AR1	1	1	1	1	**1.00**	**1**
AR2	1	1	1	1	**1.00**	**1**
AR3	1	1	1	1	**1.00**	**1**
AR4	1	1	1	1	**1.00**	**1**
AR5	1	1	1	1	**1.00**	**1**
AR6	1	1	1	1	**1.00**	**1**
AR7	2	1	2	1	**1.50**	**2**
AR8	1	1	1	1	**1.00**	**1**
SR1	1	1	1	1	**1.00**	**1**
SR2	1	1	1	1	**1.00**	**1**
SR3	1	1	1	1	**1.00**	**1**
SR4	1	1	1	1	**1.00**	**1**
SR5	1	1	1	1	**1.00**	**1**
SR7	1	1	1	1	**1.00**	**1**

is prevalent in highway scenario in 15 out of 17 receivers, and in 9 from 17 receivers in the urban scenario with smaller differences between the components.

The position availability analysis in Table 10 introduces high performances of the automotive and smartphone receivers, reaching up to 100% availability, while the geodetic receivers provided lower values at around 90%. A new methodology clarifies the reasons for low availability presented in Fig. 17 and Fig. 18. They present the availability outage distribution by grouping the outage intervals into histogram bins. The most accurate geodetic receiver GR1 has 89.33% of position losses in the upper bin with interval length of more than 10 seconds, thus massively lowering the overall availability.

Finally, the accuracy and the availability classification was performed using the COST Action SaPPART metrics. The urban environment prevents the accuracy results to fall into the most accurate classes from both perspectives: technological and application. It is evident, that for the most demanding applications, the GNSS positioning alone cannot fulfill the expected requirements in all the environments. Therefore a multi-sensor hybrid positioning must be used. The availability classification confirms that the modern automotive and smartphone receivers meet all the requirement for the best availability class at 99%. Although this is the strictest limit in classification Table 5, we propose an additional class starting at 99.9% that would differentiate receivers by another decade and support future, more demanding applications.

VII. CONCLUSION

The deployment of road ITS services requires a reliable positioning to meet the required end-to-end performance. The absence of standards and certification procedures motivated the launch of European COST Action SaPPART that delivered common methodologies for the performance validation of positioning terminals and provided support for the emerging standardization of ITS services. In the scope of scientific support, the experimental data collection campaign was initiated, following the guidelines from the EN 16803-1 norm. Our primary goal was the improvement of tentative position performance classification limits by analyzing 17 GNSS receivers with different performance expectations.

The gained results, presented in this paper through enhanced standardized methodology of performance assessment, will continue to contribute to our ongoing study of integrity metrics and classification, to the improvement of PVT error models for laboratory tests, to refinements of emerging standardization, and to the solving of positioning challenges of upcoming road ITS services.

ACKNOWLEDGMENT

The authors gratefully acknowledge the research group of the laboratory GEOLOC at the IFSTTAR, Nantes, for the provision of experimental vehicle VERT, computation of the reference trajectory, initial Matlab programming scripts, and all the expert support.

REFERENCES

[1] GSA, (2017). *GNSS Market Report*. [Online]. Available: https://www.gsa.europa.eu/system/files/reports/gnss_mr_2017.pdf
[2] J. Anderson, N. Kalra, K. Stanley, P. Sorensen, C. Samaras, and O. Oluwatola, *Autonomous Vehicle Technology: A Guide for Policymakers (RR-443-2)*, RAND Corp., Santa Monica, CA, 2016.
[3] *SaPPART Handbook: Assessment of Positioning Performance in its Applications*, COST document Action TU1302, 2017. [Online]. Available: http://www.sappart.net/wp-content/uploads/2017/ 06/ SaPPART_Handbook_final_06-2017.pdf
[4] *SaPPART White Paper: Better use of Global Navigation Satellite Systems for Safer and Greener Transport*, COST document Action TU1302, 2015. [Online]. Available: http://www.sappart.net/wp-content/uploads/2014/08/White-Paper_SaPPART_sept15.pdf
[5] M. A. Javed and E. B. Hamida, "On the interrelation of security, QoS, and safety in cooperative ITS," *IEEE Trans. Intell. Transp. Syst.*, vol. 18, no. 7, pp. 1943–1957, Jul. 2017.
[6] D. Lu, F. G. Toro, and B. Cai, "Methods for certification of GNSS-based safe vehicle localisation in driving assistance systems," in *Proc. Int. Conf. Connected Vehicles Expo (ICCVE)*, Shenzhen, China, Oct. 2015, pp. 226–231.
[7] D. Bétaille, A. Stern, M. Ortiz, and L. Ruotsalainen, "Autonomous vehicles: Get necessary redundancy in positioning with enhanced GNSS and maps," in *Proc. 24th World Congr. ITS*, Montreal, QC, Canada, Oct./Nov. 2017, pp. 1–10. [Online]. Available: http://itsworldcongress2017.org/presentations/
[8] M. Ortiz, D. Bétaille, F. Peyret, O. M. Lykkja, and S.-P. Oseth, "Assessment of end-to-end performances of a GNSS-based road user charging system based on IFSTTAR-GEOLOC and Q-Free cooperation," in *Proc. Eur. Navigat. Conf. (ENC)*, Helsinki, Finland, May/Jun. 2016, pp. 1–8.
[9] J. Wahlström, I. Skog, and P. Händel, "Smartphone-based vehicle telematics: A ten-year anniversary," *IEEE Trans. Intell. Transp. Syst.*, vol. 18, no. 10, pp. 2802–2825, Oct. 2017.
[10] M. Sysoev, A. Kos, J. Guna, and M. Pogačnik, "Estimation of the driving style based on the users' activity and environment influence," *Sensors*, vol. 17, no. 10, p. 2404, 2017.
[11] R. Öörni, E. Meilikhov, and T. O. Korhonen, "Interoperability of eCall and ERA-GLONASS in-vehicle emergency call systems," *IET Intell. Transport Syst.*, vol. 9, no. 6, pp. 582–590, Aug. 2015.
[12] D. Borio, C. Gioia, E. C. Pons, and G. Baldini, "GNSS receiver identification using clock-derived metrics," *Sensors*, vol. 17, no. 9, p. 2120, 2017.
[13] B. Hofmann-Wellenhof, H. Lichtenegger, and E. Wasle, *GNSS—Global Navigation Satellite Systems: GPS, GLONASS, Galileo, and More*. Wien, Austria: Springer-Verlag, 2008.
[14] P. D. Groves, *Principles of GNSS, Inertial, and Multisensor Integrated Navigation Systems*. London, U.K.: Artech House, 2008.
[15] P. J. G. Teunissen and O. Montenbruck, *Springer Handbook of Global Navigation Satellite Systems*. Cham, Switzerland: Springer, 2017.
[16] H. Kuusniemi, "User-level reliability and quality monitoring in satellite-based personal navigation," Ph.D. dissertation, Inst. Digit. Comput. Syst., Tampere Univ. Technology, Tampere, Finnland, 2005.
[17] D. N. Aloi, M. Alsliety, and D. M. Akos, "A methodology for the evaluation of a GPS receiver performance in telematics applications," *IEEE Trans. Instrum. Meas.*, vol. 56, no. 1, pp. 11–24, Feb. 2007.
[18] D. Margaria, E. Falletti, and T. Acarman, "The need for GNSS position integrity and authentication in ITS: Conceptual and practical limitations in urban contexts," in *Proc. IEEE Intell. Vehicles Symp. (IV)*, Dearborn, MI, USA, Jun. 2014, pp. 1384–1389.
[19] L. Ruotsalainen, "Vision-aided pedestrian navigation for challenging GNSS environments," Ph.D. dissertation, Tampere Univ. Technol., Tampere, Finnland, 2013. [Online]. Available: https://tutcris.tut.fi/portal/files/2315161/kuusniemi.pdf
[20] Z. Pan, H. Chai, and Y. Kong, "Integrating multi-GNSS to improve the performance of precise point positioning," *Adv. Space Res.*, vol. 60, no. 12, pp. 2596–2606, 2017.
[21] H. A. Msaewe, C. M. Hancock, P. A. Psimoulis, G. W. Roberts, L. Bonenberg, and H. de Ligt, "Investigating multi-GNSS performance in the UK and China based on a zero-baseline measurement approach," *Measurement*, vol. 102, pp. 186–199, May 2017.
[22] B. Bonet, I. Alcantarilla, D. Flament, C. Rodriguez, and N. Zarraoa, "The benefits of multi-constellation GNSS: Reaching up even to single constellation GNSS users," in *Proc. 22nd Int. Tech. Meeting Satell. Division Inst. Navigat. (ION GNSS)*, Savannah, GA, USA, 2009, pp. 1268–1280.

[23] Z. Jiang and P. D. Groves, "GNSS NLOS and multipath error mitigation using advanced multi-constellation consistency checking with height aiding," in *Proc. 25th Int. Tech. Meeting Satell. Division Inst. Navigat. (ION GNSS)*, Nashville, TN, USA, 2012, pp. 79–88.

[24] X. Liang, Z. Huang, H. Qin, and Y. Liu, "GNSS multi-frequency multi-system highly robust differential positioning based on an autonomous fault detection and exclusion method," *IEEE Access*, vol. 5, pp. 26842–26851, 2017.

[25] F. Khosravi, H. Moghadas, and P. Mousavi, "A GNSS antenna with a polarization selective surface for the mitigation of low-angle multipath interference," *IEEE Trans. Antennas Propag.*, vol. 63, no. 12, pp. 5287–5295, Dec. 2015.

[26] O. Julien and C. Macabiau, "Finding the right algorithm: Low-cost, single-frequency GPS/GLONASS RTK for road users," *Inside GNSS*, vol. 8, no. 6, pp. 70–80, 2013.

[27] S. K. Moore, "Super-accurate GPS coming to smartphones in 2018 [News]," *IEEE Spectr.*, vol. 54, no. 11, pp. 10–11, Nov. 2018.

[28] J. Speidel, M. Tossaint, S. Wallner, and J. A. Angclavila-Rodngucz, "Integrity for aviation: Comparing future concepts," *Inside GNSS*, vol. 8, no. 4, pp. 54–64, 2013.

[29] W. Y. Ochieng, K. Sauer, D. Walsh, G. Brodin, S. Griffin, and M. Denney, "GPS integrity and potential impact on aviation safety," *J. Navig.*, vol. 56, no. 1, pp. 51–65, 2003.

[30] *Required Navigation Performance Authorization Required (RNP AR) Procedure Design Manual*, document 9905, AN/471, International Civil Aviation Organization, Montréal, QC, Canada, 2009.

[31] *Space—Use of GNSS-Based Positioning for Road Intelligent Transport Systems (ITS), Part 1: Definitions and System Engineering Procedures for the Establishment and Assessment of Performances Solution*, document EN 16803-1:2016, CEN-CENELEC/TC5, 2016. [Online]. Available: https://www.cenelec.eu

[32] *Memorandum of Understanding*, COST document TU1302, 2013. [Online]. Available: https://e-services.cost.eu/files/domain_files/TUD/Action_TU1302/mou/TU1302-e.pdf

[33] *SaPPART Guidelines: Performance Assessment of Positioning Terminals*, COST document Action TU1302, 2018. [Online]. Available: http://www.sappart.net/wp-content/uploads/2018/04/SaPPART_Guidelines_version-web.pdf

[34] P.-Y. Gilliéron, L. Ruotsalainen, F. Peyret, S. Feng, and J. Engdahl, "The SaPPART COST Action: Towards positioning integrity for road transport," in *Proc. Eur. Navigat. Conf. (ENC)*, Helsinki, Finland, May/Jun. 2016, pp. 1–6.

[35] *u-blox M8 Receiver Description Including Protocol Specification*, document UBX-13003221, u-Blox, 2017. [Online]. Available: https://www.u-blox.com/sites/default/files/products/documents/u-blox8-M8_ReceiverDescrProtSpec_%28UBX-13003221%29.pdf

[36] N. M. Drawil, H. M. Amar, and O. A. Basir, "GPS localization accuracy classification: A context-based approach," *IEEE Trans. Intell. Transp. Syst.*, vol. 14, no. 1, pp. 262–273, Mar. 2013.

[37] P. Clausen, P.-Y. Gilliéron, H. Perakis, V. Gikas, and I. Spyropoulou, "Assessment of positioning accuracy of vehicle trajectories for different road applications," *IET Intell. Transport Syst.*, vol. 11, no. 3, pp. 113–125, Apr. 2017.

[38] J. Marais, M. Berbineau, and M. Heddebaut, "Land mobile GNSS availability and multipath evaluation tool," *IEEE Trans. Veh. Technol.*, vol. 54, no. 5, pp. 1697–1704, Sep. 2005.

[39] B. Muhammad, E. Cianca, and A. M. Salonico, "Multi GNSS advanced RAIM: An availability analysis," in *Proc. IEEE Int. Workshop Metrology for Aerosp. (MetroAeroSpace)*, Benevento, Italy, May 2014, pp. 28–33.

[40] N. Zhu, J. Marais, D. Bétaille, and M. Berbineau, "GNSS position integrity in urban environments: A review of literature," *IEEE Trans. Intell. Transp. Syst.*, to be published. [Online]. Available: https://ieeexplore.ieee.org/document/8248655/

[41] D. Borio, C. Gioia, A. Stern, F. Dimc, and G. Baldini, "Jammer localization: From crowdsourcing to synthetic detection," in *Proc. 29th Int. Tech. Meeting Satell. Division Inst. Navigat. (ION GNSS+)*, Portland, OR, USA, 2016, pp. 3107–3116.

[42] D. Borio, C. O'Driscoll, and J. Fortuny, "GNSS Jammers: Effects and countermeasures," in *Proc. 6th ESA Workshop Satell. Navigat. Technol. (Navitec) Eur. Workshop GNSS Signals Signal Process.*, Noordwijk, The Netherlands, Dec. 2012, pp. 1–7.

[43] R. H. Mitch *et al.*, (2012). Know Your Enemy: Signal Characteristics of Civil GPS Jammers, GPS World. [Online]. Available: http://gpsworld.com/gnss-systeminnovation-know-your-enemy-12475/

[44] F. Wang, H. Li, and M. Lu, "GNSS spoofing countermeasure with a single rotating antenna," *IEEE Access*, vol. 5, pp. 8039–8047, 2017.

[45] S. Han, L. Chen, W. Meng, and C. Li, "Improve the security of GNSS receivers through spoofing mitigation," *IEEE Access*, vol. 5, pp. 21057–21069, 2017.

[46] L. Heng, D. B. Work, and G. X. Gao, "GPS signal authentication from cooperative peers," *IEEE Trans. Intell. Transp. Syst.*, vol. 16, no. 4, pp. 1794–1805, Aug. 2015.

[47] Y. Cui *et al.*, "Feasibility analysis of low-cost GNSS receivers for achieving required positioning performance in CAV applications," in *Proc. Forum Cooperat. Positioning Service (CPGPS)*, May 2017, pp. 355–361.

[48] A. Steingass, B. Krach, and M. Crisci, "Robustness versus accuracy: Multipath effects on land mobile satellite navigation," *IET Radar, Sonar Navig.*, vol. 11, no. 3, pp. 520–527, Mar. 2017.

[49] K. Węzka, I. Herrera-Pinzón, and R. Galas, "Reliability monitoring of GNSS observables under the influence of ionospheric disturbances," in *Proc. IEEE/ION Position, Location Navigat.Symp. (PLANS)*, Savannah, GA, USA, Apr. 2016, pp. 431–441.

[50] European GNSS Agency, (2015). *Report on the Performance and Level of Integrity for Safety and Liability Critical Multi-Applications*. [Online]. Available: https://www.gsa.europa.eu/sites/default/files/calls_for_proposals/Annex 2.pdf

[51] K. A. Bin Ahmad, M. Sahmoudi, and C. Macabiau, "Characterization of GNSS receiver position errors for user integrity monitoring in urban environments," in *Proc. Eur. Navigat. Conf. (ENC-GNSS)*, Rotterdam, The Netherlands, 2014, pp. 1–15.

[52] D. Betaille, F. Peyret, M. Ortiz, S. Miquel, and L. Fontenay, "A new modeling based on urban trenches to improve gnss positioning quality of service in cities," *IEEE Intell. Transp. Syst. Mag.*, vol. 5, no. 3, pp. 59–70, Jul. 2013. [Online]. Available: https://ieeexplore.ieee.org/document/6565516/, doi: 10.1109/MITS.2013.2263460.

[53] C. Basnayake, T. Williams, P. Alves, and G. Lachapelle, (2010). Can GNSS Drive V2X? GPS World. [Online]. Available: http://gpsworld.com/transportationroadcan-gnss-drive-v2x-10611/

[54] S. Stephenson, X. Meng, T. Moore, A. Baxendale, and T. Edwards, "Accuracy requirements and benchmarking position solutions for intelligent transportation location based services," in *Proc. 8th Symp. Location Based Services*, Vienna, Austria, 2011, pp. 21–23.

[55] M. Kirkko-Jaakkola *et al.*, "Effect of antenna location on GNSS positioning for ITS applications," in *Proc. Eur. Navigat. Conf. (ENC)*, Helsinki, Finland, May/Jun. 2016, pp. 1–7.

[56] J. Januszewski, "Visibility of satellites and their geometry for different numbers of satellites of global navigation systems," in *Proc. 17th Int. Conf. Transport Syst. Telematics (TST)*, vol. 715, Katowice, Poland, 2017, pp. 260–270.

[57] D. Borio, F. Dovis, H. Kuusniemi, and L. Lo Presti, "Impact and detection of GNSS jammers on consumer grade satellite navigation receivers," *Proc. IEEE*, vol. 104, no. 6, pp. 1233–1245, Jun. 2016.

[58] A. Martellucci and R. P. Cerdeira, "Review of tropospheric, ionospheric and multipath data and models for global navigation satellite systems," in *Proc. Eur. Conf. Antennas Propag. (EuCAP)*, Berlin, Germany, Mar. 2009, pp. 3697–3702.

[59] X. Yue *et al.*, "The effect of solar radio bursts on the GNSS radio occultation signals," *J. Geophys. Res., Space Phys.*, vol. 118, no. 9, pp. 5906–5918, Sep. 2013.

[60] F. Peyret, "Standardization of performances of GNSS-based positioning terminals for ITS applications at CEN/CENELEC/TC5," in *Proc. 20th World Congr. Intell. Transport Syst.*, Tokio, Japan, 2013, pp. 1–10.

[61] C. Cristodaro, F. Dovis, G. Falco, and M. Pini, "GNSS receiver performance in urban environment: Challenges and test approaches for automotive applications," in *Proc. Int. Conf. Elect. Electron. Technol. Automot.*, Torino, Italy, Jun. 2017, pp. 1–6.

[62] Septentrio Satellite Navigation, (2011). *AsteRx3: GNSS Multi-Frequency Receiver*. [Online]. Available: http://www.terri sgps.com/product_files/septentrio-asterx3-datasheet_343.pdf

[63] Novatel, (2011). *DL-V3 Product Sheet*. [Online]. Available: https://www.novatel.com/assets/Documents/Papers/DL-V3.pdf

[64] V. Renaudin and D. Betaille, "From lab to road test," *Inside GNSS*, vol. 8, no. 5, pp. 42–60, Sep./Oct. 2013.

[65] V. Gikas and H. Perakis, "Rigorous performance evaluation of smartphone GNSS/IMU sensors for ITS applications," *Sensors*, vol. 16, no. 8, p. E1240, 2016.

[66] S. Pullen, "Quantifying the performance of navigation systems and standards for assisted-GNSS," *Inside GNSS*, vol. 3, no. 6, pp. 20–24, Sep./Oct. 2008.

ANDREJ ŠTERN received the M.S. degree in electrical engineering from the University of Ljubljana, Slovenia, in 2003. He is currently a Senior Lecturer with the Faculty of Electrical Engineering, University of Ljubljana, where he is a member of the Laboratory for Telecommunications, Department of Information and Communication Technologies. He has authored or co-authored 36 conference papers and holds seven patents. His teaching and research work includes mobile networks and technologies, sensor networks, embedded systems, Internet of Things, satellite navigation, and vehicle telematics. He is an Active Member of the Slovenian ITS Association, a member of the Program Committee of International Symposium on Electronics in Transport, and a Management Committee Member of an European COST Action TU1302-SaPPART.

ANTON KOS (M'98–SM'17) received the Ph.D. degree in electrical engineering from the University of Ljubljana, Slovenia, in 2006. He is currently an Associate Professor with the Faculty of Electrical Engineering, University of Ljubljana, where he is a member of the Laboratory of Information Technologies, Department of Information and Communication Technologies. He has authored or co-authored 27 papers appeared in the international engineering journals and over fifty papers in international conferences. His teaching and research work includes communication networks and protocols, quality of service, dataflow computing and applications, usage of sensors in biofeedback systems and applications, signal processing, and information systems. He has been an IEEE Slovenia ComSoc Chapter Chair since 2018.